Adiabatic quantum pumping in an Aharonov-Bohm loop and in a siliconlike nanowire: The role of interference in position space and in momentum space

Sungjun Kim,[1] Kunal K. Das,[2] and Ari Mizel[1]
[1]*Department of Physics, The Pennsylvania State University, University Park, Pennsylvania 16802, USA*
[2]*Department of Physics, Fordham University, Bronx, New York 10458, USA*
(Received 25 September 2006; revised manuscript received 2 March 2007; published 7 August 2007)

We study the consequences of interference effects on the current generated by adiabatic quantum pumping in two distinct one-dimensional lattice models. The first model contains an Aharonov-Bohm (AB) loop within a tight-binding chain of lattice sites. The static AB phase is shown to strongly affect interference between the two arms of the loop, serving as an on-off switch and regulator for the pumped current. The second model simulates pumping in semiconductors with indirect band gaps by utilizing a tight-binding chain with next-nearest-neighbor coupling. The model exhibits signatures of interference between degenerate conduction band states with different Fermi wave vectors.

DOI: 10.1103/PhysRevB.76.085307 PACS number(s): 73.23.−b, 73.63.−b, 72.10.Bg, 72.80.Cw

I. INTRODUCTION

Adiabatic quantum pumping provides a mechanism to generate a direct current with no bias.[1] By periodically changing the parameters that define a conduction channel, one forces carriers down the channel. The quantity of pumped carriers depends only on the path that the parameters take through parameter space and not on the speed with which this path is traversed[2] (as long as the change is slow enough to remain adiabatic). Recently, adiabatic quantum pumping has been applied to a number of different transport contexts, including the generation of spin polarized current[3–9] and entangled pairs.[10–12] Experiments continue to be motivated by sustained interest in this unusual mesoscopic transport mechanism.[5,13,14]

Since pumping itself is a consequence of quantum interference, it is of interest to see how it is affected by other quantum interference phenomena working in conjunction. In this work, we study two pump configurations which create additional interference effects (i) due to differences in spatial trajectories and (ii) due to competing momenta. It is natural to think of the former as an interference effect in position space and the latter as an interference effect in momentum space.

The first configuration comprises of an Aharonov-Bohm (AB) loop geometry, which is the subject of many studies associated with AB phase effects and Fano effects.[15–18] A pair of parallel quantum dots straddling a linear chain of dots serve as the two arms of an AB loop. Differences in spatial trajectories are created in the two arms of the loop. We find surprising sensitivity of the pumped charge to the presence and magnitude of a *static* magnetic field associated with the AB effect; even with two time varying and out of phase parameters, there is no pumped current when the field is absent.

Early experimental work on adiabatic quantum pumping[19] observed a pumped current that is symmetric under magnetic field reversal, while theory predicted no definite symmetry.[20] It was suggested that the observed currents may be due to rectification effects rather than pumping.[21] It is thus desirable to have a model in which pumped current and rectification current can be definitively distinguished. Since rectification currents should be symmetric under magnetic field reversal, our model is designed to have a mirror symmetry that causes the pumped charge to be antisymmetric $q_{pump}(-B) = -q_{pump}(B)$ under magnetic field reversal. Thus, in an experimental realization of the model, a current observed to be antisymmetric under magnetic field reversal could be due to quantum pumping, while deviation from antisymmetry would indicate another mechanism at work.

The second model that we consider is a tight-binding chain with next-nearest-neighbor (nnn) hopping; in the presence of such hopping, the conduction band energy need not lie at $k=0$, and the conduction band can look like that of a semiconductor with an indirect gap. A physical motivation for this model is the band structure of Si nanowires. Calculations have predicted an indirect gap[22] when Si nanowires are grown along certain directions, say, the $[11\bar{2}]$ direction. The conduction band dispersion relation in our model can have four Fermi wave vectors at a given Fermi energy E_F. Our calculations show rich interference effects between these wave vectors, including resonant peaks of different heights in the pumped current.

The rest of the paper is organized as follows. In Sec. II, we formulate our method for computing the current pumped in a one-dimensional lattice due to an arbitrary localized time-varying potential. In Sec. III, we compute the effects of a static magnetic field on the AB loop system and demonstrate the spatial interference effects induced by that field on the pumped current. We study the effects of nnn coupling in Sec. IV and analyze wave vector interference phenomena. We summarize our primary conclusions in Sec. V.

II. MECHANISM OF ADIABATIC PUMPING IN A ONE-DIMENSIONAL CHAIN

The description of adiabatic pumping in mesoscopic systems is based on the Landauer-Büttiker scattering picture. For a single channel in a system describable by a one-dimensional lattice Hamiltonian, the instantaneous pumped current is[9,23]

$$j_{pump}(n) = e \int dE f(E) \int_{-\pi}^{\pi} \frac{dp}{2\pi} \delta(E - E_p) \langle \phi_p | j_n | \phi_p \rangle, \quad (1)$$

where j_n is the appropriate discrete current operator for the one-dimensional chain. The system has a single Fermi distribution function $f(E)$, since pumping operates in the absence of bias. The matrix elements of the current operator are taken with respect to scattering states $|\phi_p(t)\rangle$ of the full *time-dependent* Hamiltonian $H(t)$ of the system. When the time dependence of the Hamiltonian is adiabatic, the states $|\phi_p(t)\rangle$ can be approximated by an expansion in terms of the *instantaneous* scattering states $|\chi_p(t)\rangle$ up to linear order in the time derivative,

$$|\phi_p(t)\rangle = |\chi_p(t)\rangle - i\hbar G(E_p)|\dot{\chi}_p(t)\rangle. \quad (2)$$

Here, $G(E_p) = 1/(E_p - H + i\eta)$ is the retarded Green's function for the instantaneous Hamiltonian H with $\eta = 0^+$ imposing causality. The instantaneous scattering states

$$|\chi_p(t)\rangle = (1 + G(E_p)V)|p\rangle \quad (3)$$

are exact solutions to the Lippmann-Schwinger equation for the instantaneous scattering potential V that contains the time-varying part of the full Hamiltonian H. (Here, $|p\rangle$ is a plane wave state.) If the time dependence in H is not explicit but instead arises only through time-dependent parameters, the states $|\phi_p(t)\rangle$ and $|\chi_p(t)\rangle$ inherit time dependence through those parameters and also do not explicitly depend on time.

We apply the above considerations to a one-dimensional (1D) lattice Hamiltonian comprising of the standard time-independent tight-binding Hamiltonian H_0 with nearest-neighbor coupling and a general time-dependent potential $V(t)$ acting on a finite "scattering region" of the lattice:

$$H(t) = H_0 + V(t),$$

$$H_0 = -J \sum_n (a_{n+1}^\dagger a_n + a_n^\dagger a_{n+1}),$$

$$V(t) = \sum_{x,y} V_{xy}(t) a_x^\dagger a_y. \quad (4)$$

Here, $a_n^\dagger$ is the electron creation operator at site n and $-J$ is the nearest-neighbor hopping coupling strength. The on-site energy of the sites of the free Hamiltonian H_0 is taken to be the reference energy and hence set to zero. The potential $V(t)$ is parametrized by the $V_{xy}(t)$ which contribute to the intersite coupling strengths $(x \neq y)$ and on-site energy shifts $(x = y)$ within the scattering region. Since the current is always defined asymptotically far from the scattering region, H_0 determines the definition of the current operator

$$j_n = -\frac{J}{i\hbar}(a_{n+1}^\dagger a_n - a_n^\dagger a_{n+1}), \quad (5)$$

as well as the dispersion relation $E_p = -2J \cos p$, where the spacing between the sites in the chain has been set to unity, thereby setting a natural length scale.

We evaluate the pumped current for this Hamiltonian in the distant region $n \to \infty$ through an adaptation of an analysis we presented in a recent publication.[9] We only consider real pumping parameters in this paper, so we set $\dot{V}_{xy} = \dot{V}_{yx}$ for all x, y. The pumped current for the time-dependent Hamiltonian in Eq. (4) is then given by

$$j_{pump}(n) = -\frac{eJ}{\pi} \int dE f(E) \mathrm{Im} \sum_{x,y} \dot{V}_{xy} \partial_E [G^*(E)(n+1,x) \times G(E)(n,y)]. \quad (6)$$

We use here the notation $G(E)(n,x) = \langle 0 | a_n G(E) a_x^\dagger | 0 \rangle$. Since pumping experiments require low temperatures, we take the zero temperature limit whereby $f(E)$ becomes a step function and an integration by parts transforms Eq. (6) for the pumped current to

$$j_{pump}(n) = -\frac{eJ}{\pi} \mathrm{Im} \sum_{x,y} \dot{V}_{xy} G^*(E_F)(n+1,x) G(E_F)(n,y), \quad (7)$$

where $G(E_F)(n,x)$ is the full propagator in the energy domain evaluated at the Fermi energy. We will take our time-varying parameters to be on-site energies, so only the diagonal elements of V_{xy} will have nonvanishing time derivatives and we simplify the notation by defining $\dot{V}_{xy} = \dot{u}_x \delta_{x,y}$. Using Dyson's equation,[24] $G(E) = G_0(E) + G_0(E) V G(E)$, where $G_0(E) = 1/(E - H_0 + i\eta)$, we can show that $G(E_F)(n,x) = -2\pi i N(E_F)[e^{ik_F(n-x)} + \Sigma_{x'} u_{x'} e^{ik_F(n-x')} G(E_F)(x',x)]$ for n larger than all x, x' in the scattering region. Thus, we have the identity $G(E_F)(n+1,x) = e^{ik_F} G(E_F)(n,x)$ for n larger than all x in the scattering region, and expression (7) for the pumped current becomes

$$j_{pump}(n) = \frac{e}{(2\pi)^2} N(E_F)^{-1} \sum_x \dot{u}_x |G(E_F)(n,x)|^2, \quad (8)$$

with $N(E_F) = \frac{1}{2\pi} \frac{\partial k}{\partial E_k}\big|_{k=k_F}$ being the one-dimensional density of states per unit length. In fact, using Dyson's equation result, one can show that the current is independent of the site index n as one should expect from charge conservation,

$$j_{pump} = eN(E_F) \sum_x \dot{u}_x \left| 1 + \sum_{x'} u_{x'} e^{-ik_F(x'-x)} G(E_F)(x',x) \right|^2. \quad (9)$$

In this expression, the instantaneous pumped current is determined by the density of states, instantaneous potentials and their time derivatives, and the *local* full propagator (local since x and x' are both in the scattering region where u_x and $u_{x'}$ are both nonzero), which can be determined from Dyson's equation from a knowledge of the potential and the free Green's function.

III. PUMPING THROUGH A LOOP GEOMETRY

We now apply the considerations of the previous section to determine the pumped current for our first physical model of interest, consisting of a 1D tight-binding chain with a loop in the central region as shown in Fig. 1. The Hamiltonian has

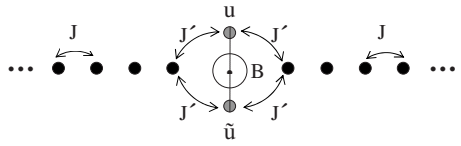

FIG. 1. Two quantum dots are connected to left and right leads in parallel. They form a closed loop in the central region, which is threaded by a magnetic field B. One dot has on-site energy u and the other has on-site energy $\tilde{u}$. The symbols $-J$ and $-J'$ are hopping amplitudes. The vertical line shows the plane of left-right reflection symmetry when $B=0$.

the general form shown in Eq. (4) where the potential is now specifically

$$V(t) = u(t)b_0^\dagger b_0 + \tilde{u}(t)\tilde{b}_0^\dagger \tilde{b}_0 + J[a_0^\dagger a_{-1} + a_1^\dagger a_0] - J' e^{i\varphi/4}[\tilde{b}_0^\dagger a_{-1} + a_1^\dagger \tilde{b}_0] - J' e^{-i\varphi/4}[b_0^\dagger a_{-1} + a_1^\dagger b_0] + (\text{H.c.}). \quad (10)$$

To obtain this potential, we imagine displacing site 0 above the chain so that it forms the upper arm of a loop. We define the creation operator $b_0^\dagger \equiv a_0^\dagger$, introducing new notation for the displaced state. We introduce a new site to form the lower arm; the creation operator associated with this new site is $\tilde{b}_0^\dagger$. Thus, the two parallel sites in the middle of the chain are represented by $b_0^\dagger$ and $\tilde{b}_0^\dagger$. These sites are decoupled from each other but are coupled to the rest of the chain on either side with a coupling strength of $-J'$. The two sites straddling the chain create a loop, and a static magnetic flux Φ penetrating that loop creates an Aharonov-Bohm phase difference $\varphi = 2\pi\Phi/\Phi_0$, where $\Phi_0 = hc/e$, between the two spatial paths defined by the arms of the loop, leading to interference effects. In our model, the time dependence lies at the on-site energies of the two parallel sites $\tilde{u}$ and u, which serve as the pumping parameters. (Single parameter pumping in the loop geometry was studied in Ref. 25, where the pumped current was evaluated in a second order calculation.)

By specifying a cyclic time dependence of the parameters u and $\tilde{u}$, we can integrate the expression in Eq. (9) to compute the charge pumped in a full cycle,

$$q_{pump} = \oint dt j_{pump}(n). \quad (11)$$

We choose a simple square-loop time cycle as shown in Fig. 2(b) in the space of the two pumping parameters. The charge pumped over a cycle is computed numerically, and the behavior as a function of the Aharonov-Bohm phase φ is presented in Fig. 2(a). The dependence as a function of the Fermi vector k_F is shown in Fig. 3. The results show several interesting features that we now discuss in detail.

(i) The current vanishes in the absence of the static magnetic field. The magnetic field plays a crucial role even though it does not vary in time and therefore never acts as a pumping parameter. The necessity for the static magnetic field can be understood by recognizing that our system has reflection symmetry about a plane through the two loop sites, orthogonal to the direction of flow. It is easy to see by simply

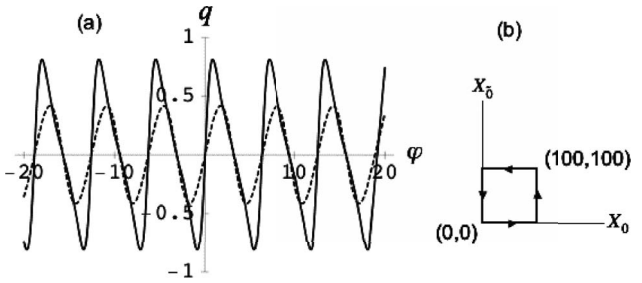

FIG. 2. (a) Charge q (in units of e throughout paper) pumped per cycle vs φ (in radians): We set $J'/J=0.5$ and traverse a square-shaped pumping cycle with corners $(X_0, X_{\tilde{0}}) = (u/J, \tilde{u}/J) = (0,0)$ and (100, 100) as shown in (b). The solid line in (a) is for $k_F=1.7$, and the dashed line is for $k_F=2.1$. This plot shows the antisymmetry and periodicity of the pumped charge as a function of the magnetic field. The slope of the solid line near the origin indicates a pumped current that is highly sensitive to small magnetic fields.

reversing the magnetic field, and simultaneously exchanging sites n with $-n$, that the reflection symmetry implies

$$\oint dt j_{pump}(n,-\varphi) = -\oint dt j_{pump}(n,\varphi). \quad (12)$$

This is an example of a discrete symmetry[20] which causes the pumped charge to be antisymmetric under reversal of magnetic field. This antisymmetry is also manifested in Fig. 3, where the two traces of the pumped charge, as a function of the Fermi vector k_F, are exactly antisymmetric because one is for $\varphi=\pi/2$ and the other is for $\varphi=3\pi/2\equiv-\pi/2$.

More intuitively, when the magnetic field is absent, the two parallel quantum dots effectively pump at the same location along the current flow. The two potentials combine into a single parameter, and a single parameter cannot pump any current within our adiabatic calculation. The static magnetic field breaks the reflection symmetry and creates a phase shift between the two dots. They no longer lie symmetrically at the same location in the current flow and now act as two separate pumping parameters, producing a current. In Ref. 26, a related effect was seen in a very different configuration

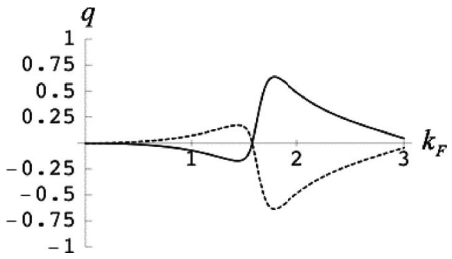

FIG. 3. Pumped charge q vs k_F: We set $J'/J=0.5$ and traverse a square-shaped pumping cycle with corners $(X_0, X_{\tilde{0}}) = (0,0)$ and (100, 100). The solid line is for $\varphi=\frac{\pi}{2}$, which corresponds to $\Phi=\frac{1}{4}\Phi_0$, and the dashed line is for $\varphi=\frac{3\pi}{2}$, which corresponds to $\Phi=\frac{3}{4}\Phi_0$. Since the current is periodic for φ and is antisymmetric when the sign of φ is reversed, the two curves shown have opposite values of pumped charge at any given k_F.

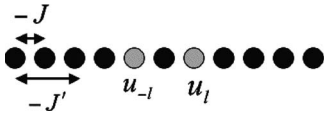

FIG. 4. We consider a 1D tight-binding chain with both nearest-neighbor and next-nearest-neighbor couplings, where $-J$ is the strength for nearest-neighbor hopping and $-J'$ is the strength for next-nearest-neighbor hopping. On this chain, we assume that only two sites (gray dots) located at $-l$ and l have nonzero on-site energies u_{-l}, u_l.

involving two loops where the pumping parameters were time-varying magnetic fields. In that work, the static field also breaks the symmetry, allowing a pumping current to arise.

(ii) There is a periodicity in the charge pumped with respect to the phase introduced by the static magnetic field, as shown in Fig. 2. This periodicity is an expected feature of AB phenomena. The periodicity of $\varphi=2\pi$ causes the pumped charge to vanish when the phase difference due to the magnetic field between the two arms of the loop vanishes, equivalent to having no field at all.

(iii) The pumped charge also vanishes for $k_F=n\pi/2$. This can be seen in Fig. 3, where the pumped charge is plotted as a function of k_F for two different values of the Aharonov-Bohm phase φ. The reason is that an electron picks up a phase of $\pm k_F$ as it moves from site to adjacent site. Therefore, in traversing one of the arms of the loop, it picks up a total phase of $\pm 2k_F \pm \varphi/2$, and in going through the other arm, the corresponding total phase change is $\mp 2k_F \mp \varphi/2$. When $k_F = \pi/2$, they become, respectively, $\pm\pi\pm\varphi/2$ and $\mp\pi\mp\varphi/2 \equiv 2\pi-(\mp\pi\pm\varphi/2)\equiv\pm\pi\pm\varphi/2$. This shows that the phases accumulated in both paths are identical, and therefore, the symmetry-breaking effect of the magnetic field is annulled and the pumped charge vanishes as if the magnetic field were not there at all.

We conclude the discussion of this system by noting that the pumped current is quite sensitive to changes in the external magnetic field as seen from the solid curve in Fig. 2(a). This can provide a way of precisely controlling the magnitude and direcltion of the pumped current without changing the time-varying pumping parameters in any way. In addition, the fact that the absence of the field leads to vanishing current suggests application of this model as a switching mechanism.

IV. PUMPING ON A CHAIN WITH NEXT-NEAREST-NEIGHBOR HOPPING

We now turn our attention to the pumped current on a chain with next-nearest-neighbor (nnn) hopping (see Fig. 4). We consider the following Hamiltonian:

$$H(t) = H_0 + V(t),$$

$$H_0 = -J\sum_n (a_{n+1}^\dagger a_n + a_n^\dagger a_{n+1}) - J'\sum_n (a_{n+2}^\dagger a_n + a_n^\dagger a_{n+2}),$$

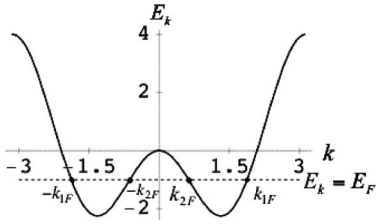

FIG. 5. The dispersion relation when the energy J is set to 1 and the energy J' is set to -1. It has a double-well shape. The dashed line is for $E_k=E_F=-1$; it has four crossing points with the double-well curve, corresponding to four Fermi wave vectors $\{k_{1F}, k_{2F}, -k_{1F}, -k_{2F}\}$.

$$V(t) = u_{-l}(t)n_{-l} + u_l(t)n_l, \tag{13}$$

where $-J'$ is the nnn hopping amplitude and $n_l=a_l^\dagger a_l$ is the number operator on site l. The on-site energy is taken to be zero for all sites except for the sites $\pm l$. The energies at those sites u_l and u_{-l} are the time-varying pumping parameters.

The dispersion relation for this model (taking the lattice constant to be unity) is $E_k=-2J\cos k-2J'\cos 2k$. We assume a positive J and negative J' so that the dispersion relation yields a double-well shape as shown in Fig. 5. This "indirect gap" shape is physically relevant, being reminiscent, for instance, of the band structure of certain Si nanowires.[22] For any total energy $J^2/(4J')+2J'<E<0$ in Fig. 5, solving $E_k=E$ yields four solutions $\{\pm k_1(E), \pm k_2(E)\}$, related by $\cos k_1+\cos k_2=-J/(2J')$. At zero temperature, the pumping dynamics is determined by the Fermi energy $E=E_F$; we denote the corresponding wave vectors $\{\pm k_{1F}, \pm k_{2F}\}$. We choose the convention that $k_1>k_2>0$.

We need to extend the analysis of Sec. II to get the pumped current by defining an appropriate discrete current operator for this extended chain. Since there is a nnn hopping process, we define the current operator using the continuity equation $\partial_t[\rho(n)+\rho(n+1)]+J(n+1)-J(n-1)=0$, where $\rho(n)=\langle\psi|a_n^\dagger a_n|\psi\rangle$ and $J(n)=\langle\psi|J_n|\psi\rangle$. We are led to the definition of the operator

$$J_n = -\frac{J}{i\hbar}(a_{n+1}^\dagger a_n - a_n^\dagger a_{n+1}) - \frac{J'}{i\hbar}(a_{n+1}^\dagger a_{n-1} - a_{n-1}^\dagger a_{n+1}) - \frac{J'}{i\hbar}(a_{n+2}^\dagger a_n - a_n^\dagger a_{n+2}). \tag{14}$$

We compute the pumped current using this current operator in the expression for the current [Eq. (1)], instead of j_n. (No confusion should arise between the current operator J_n and the tunneling parameters J and J'.) In the zero temperature limit and at points far away ($n\to\infty$) from the action of the pumping potential, the pumped current is

$$J_{pump}(n) = e\int dE f(E)\int_{-\pi}^{\pi}\frac{dp}{2\pi}\delta(E-E_p)\langle\phi_p|J_n|\phi_p\rangle$$

$$= -\frac{eJ}{\pi}\,\mathrm{Im}\sum_{x=\pm l}\dot{u}_x G(E_F)(n,x)G^*(E_F)(n+1,x)$$

$$-\frac{eJ'}{\pi}\,\mathrm{Im}\sum_{x=\pm l}\dot{u}_x G(E_F)(n-1,x)G^*(E_F)(n+1,x)$$

$$-\frac{eJ'}{\pi}\,\mathrm{Im}\sum_{x=\pm l}\dot{u}_x G(E_F)(n,x)G^*(E_F)(n+2,x). \tag{15}$$

Some care is needed in applying Eq. (15). Because of the shape of the dispersion relation, the velocity $v_k=\frac{1}{\hbar}\frac{\partial E_k}{\partial k}$ for $+k_2$ is negative while the velocity for $-k_2$ is positive. Thus, incoming waves from the left reservoir correspond to wave vectors $\{k_1,-k_2\}$ rather than $\{k_1,k_2\}$. To keep this straight, when computing the full Green's function $G(E)=1/(E-H+i\eta)$, we use $\eta=\eta_1=0^+$ at the k_1 singularity in the denominator and $\eta=\eta_2=0^-$ at the k_2 singularity in the denominator. As a result, left incoming waves with k_1 or $-k_2$ have transmitted waves with the correct physical wave vectors $\{k_1, -k_2\}$ and reflected waves with the correct physical wave vectors $\{-k_1,k_2\}$.

Using Dyson's equation to compute the full Green's function, we derive an explicit expression for the instantaneous pumped current,

$$\begin{aligned}J_{pump}=-\frac{2eJ'}{\pi}\sum_{x=\pm l}\dot{u}_x\,[g_1^2|d(-x)+e^{2ik_1x}h(-x)|^2\sin k_1\\ \times(\cos k_1-\cos k_2)+g_2^2|d(-x)+e^{-2ik_2x}h(-x)|^2\\ \times\sin k_2(\cos k_1-\cos k_2)]|_{E=E_F},\end{aligned} \tag{16}$$

where

$$d(x)=\frac{1-u_xG_0(E)(0,0)}{Z_x}, \tag{17a}$$

$$h(x)=\frac{u_xG_0(E)(x,-x)}{Z_x}, \tag{17b}$$

$$\begin{aligned}Z_x=[1-u_xG_0(E)(0,0)][1-u_{-x}G_0(E)(0,0)]\\ -u_{-x}u_xG_0^2(E)(x,-x),\end{aligned} \tag{17c}$$

$$g_1=\frac{1}{2iJ\sin k_1+4iJ'\sin 2k_1}, \tag{17d}$$

$$g_2=-\frac{1}{2iJ\sin k_2+4iJ'\sin 2k_2}, \tag{17e}$$

$$G_0(E)(x,y)=g_1e^{ik_1|x-y|}+g_2e^{-ik_2|x-y|}. \tag{17f}$$

The free Green's function $G_0(E)(x,y)$ is found to be the sum of two terms $g_1e^{ik_1|x-y|}$ and $g_2e^{-ik_2|x-y|}$. As a result, interference effects arise between the two wave vectors $\{k_1,-k_2\}$. In particular, the $G_0^2(E)(x,-x)$ term in Z_x, defined above, contains a factor of the form $e^{2i(k_1-k_2)|x|}$, which depends on the sum of the two wave vectors k_1 and $-k_2$ and the distance $2|x|$ between the locations of the two time-varying sites n_l and n_{-l} in the potential $V(t)$. This factor of $e^{2i(k_1-k_2)|x|}$ admits an interpretation in terms of interference between the wave function with vector k_1 and the one with vector $-k_2$. Physically speaking, the dependence of the pumped current on the separation $2|x|=2l$ between the two points of action of the potentials in V depends not only on k_1 and $-k_2$ individually but also on k_1-k_2. This leads to a rather irregular pattern for the pumped current as function of the separation $2l$ as seen in Fig. 6(b). This is quite distinct from the regular pattern, shown in Fig. 6(a) for comparison, for standard nearest-neighbor coupling, i.e., when $J'=0$. In all cases, u_l and u_{-l} trace out a square-shaped time cycle like the one shown in Fig. 2.

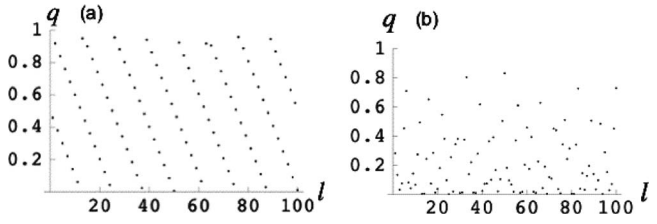

FIG. 6. Pumped charge q vs l [there is exactly one value of q for each choice of l in both (a) and (b)]. In both (a) and (b), the Fermi level is $E_F=-1.5$, and the pumping cycle is square shaped with lower-left corner (0, 0) and upper-right corner (100, 100). The distance between the two time-dependent potentials is $2l$. (a) Standard chain with $J=1$ and no nnn hopping, $J'=0$. A regular periodicity is evident. (b) Chain with nnn hopping, $J=1$ and $J'=-1$. The dependence of q on l is quite irregular with no obvious pattern.

In Fig. 7, we investigate how the pumped current depends on the Fermi wave vector k_{1F}; note that k_{1F} determines the Fermi energy E_F, via the dispersion relation, as well as $-k_{2F}$. The high peak near $k_{1F}=1.9$ results from a resonance effect, as we now explain. Note that the transmission will be greatest when the denominator Z_l, given by Eq. (17c), is as small as possible. For large u_l,u_{-l}, this means minimizing the terms in Z_l that are multiplied by the product u_lu_{-l}. This leads to the condition $G_0^2(E)(l,-l)-G_0^2(E)(0,0)=0$, which corresponds to three resonance conditions for the wave vectors: $e^{4ik_{1F}l}=1$, $e^{-4ik_{2F}l}=1$, and $e^{2i(k_{1F}-k_{2F})l}=1$. Now, when the Fermi wave vector is close to $k_{1F}\simeq 1.9$, where the strong peak occurs in Fig. 7, all three conditions are satisfied and a large pumped charge $q\simeq 1$ arises. In case of the smaller peak between $k_{1F}=1.7$ and $k_{1F}=1.8$ in Fig. 7, the value of k_{1F} satisfies the first two resonance conditions but not the third. Physically, this can be interpreted as destructive interference between the two wave vectors, resulting in a smaller pumped charge.

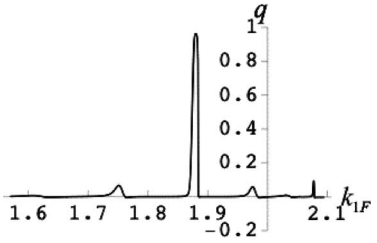

FIG. 7. Pumped charge q vs k_{1F}: We set $J=1$, $J'=-1$, and $l=10$ and use a square-shaped pumping cycle with left-lower corner at (4, 4) and right-upper corner at (100, 100). High peak near $k_{1F}=1.9$ is related to resonant transmission, and low peak between $k_{1F}=1.7$ and $k_{1F}=1.8$ indicates destructive interference between two wave vectors.

V. CONCLUSION

We have used two distinct physically relevant models to illustrate how the charge pumped in an adiabatic pumping process can be strongly influenced by interference effects in both position space and momentum space. Specifically, we have demonstrated that pumped current can be generated using a single Aharonov-Bohm loop provided a static magnetic field is present. Although that field itself is not an active pumping parameter, the pumped charge is very sensitive to its magnitude and direction, a feature that can be used for very delicate control of the pumping process. As we noted, the fact that the pumped current is antisymmetric in the magnetic field suggests an experimental means of clearly distinguishing pumped current and current arising in another way that lacks this antisymmetry. Using a next-nearest-neighbor-coupling lattice model to simulate the indirect gap present in the band structure of Si, we demonstrated that interference effects in momentum space cause strong and weak resonant peaks in the pumped current per cycle. The models considered here demonstrate that interference phenomena provide powerful techniques for altering adiabatic pumping behavior.

ACKNOWLEDGMENTS

We gratefully acknowledge the support of the Packard Foundation, NSF NIRT program Grant No. DMR-0103068, and the Research Corporation.

[1] P. W. Brouwer, Phys. Rev. B **58**, R10135 (1998).
[2] B. L. Altshuler and L. I. Glazman, Science **283**, 1864 (1999).
[3] P. Sharma and C. Chamon, Phys. Rev. Lett. **87**, 096401 (2001).
[4] E. R. Mucciolo, C. Chamon, and C. M. Marcus, Phys. Rev. Lett. **89**, 146802 (2002).
[5] S. K. Watson, R. M. Potok, C. M. Marcus, and V. Umansky, Phys. Rev. Lett. **91**, 258301 (2003).
[6] T. Aono, Phys. Rev. B **67**, 155303 (2003).
[7] Y. Wei, L. Wan, B. Wang, and J. Wang, Phys. Rev. B **70**, 045418 (2004).
[8] M. Blaauboer and C. M. L. Fricot, Phys. Rev. B **71**, 041303(R) (2005).
[9] S. Kim, K. K. Das, and A. Mizel, Phys. Rev. B **73**, 075308 (2006).
[10] C. W. J. Beenakker, M. Titov, and B. Trauzettel, Phys. Rev. Lett. **94**, 186804 (2005).
[11] P. Samuelsson and M. Büttiker, Phys. Rev. B **71**, 245317 (2005).
[12] K. K. Das, S. Kim, and A. Mizel, Phys. Rev. Lett. **97**, 096602 (2006); K. K. Das, S. Kim, and A. Mizel, Bull. Am. Phys. Soc. **49**, 218 (2004).
[13] L. DiCarlo, C. M. Marcus, and J. S. Harris, Jr., Phys. Rev. Lett. **91**, 246804 (2003).
[14] M. R. Buitelaar, P. J. Leek, V. I. Talyanskii, C. G. Smith, D. Anderson, G. A. C. Jones, J. Wei, and D. H. Cobden, Semicond. Sci. Technol. **21**, S69 (2006).
[15] Y. Gefen, Y. Imry, and M. Ya. Azbel, Phys. Rev. Lett. **52**, 129 (1984).
[16] K. Kobayashi, H. Aikawa, S. Katsumoto, and Y. Iye, Phys. Rev. Lett. **88**, 256806 (2002).
[17] A. Aharony, O. Entin-Wohlman, and Y. Imry, Phys. Rev. Lett. **90**, 156802 (2003).
[18] H. Lu, R. Lü, and B. Zhu, Phys. Rev. B **71**, 235320 (2005).
[19] M. Switkes, C. M. Marcus, K. Campman, and A. C. Gossard, Science **283**, 1905 (1999).
[20] I. L. Aleiner, B. L. Altshuler, and A. Kamenev, Phys. Rev. B **62**, 10373 (2000).
[21] P. W. Brouwer, Phys. Rev. B **63**, 121303(R) (2001).
[22] H. Scheel, S. Reich, and C. Thomsen, Phys. Status Solidi B **242**, 2474 (2005).
[23] O. Entin-Wohlman, A. Aharony, and Y. Levinson, Phys. Rev. B **65**, 195411 (2002).
[24] E. N. Economou, *Green's Functions in Quantum Physics* (Springer-Verlag, Berlin, 1979).
[25] L. E. F. Foa Torres, Phys. Rev. B **72**, 245339 (2005).
[26] D. Shin and J. Hong, Phys. Rev. B **70**, 073301 (2004).